

JAERI - M
87-064

A SIMPLE MODEL FOR HOT ION PLASMAS

May 1987

P. R. Thomas*

JAERI-M レポートは、日本原子力研究所が不定期に公刊している研究報告書です。
入手の問合わせは、日本原子力研究所技術情報部情報資料課（〒319-11 茨城県那珂郡東海村）
あて、お申しこしてください。なお、このほかに財団法人原子力弘済会資料センター（〒319-11 茨城
県那珂郡東海村日本原子力研究所内）で複写による実費頒布をおこなっております。

JAERI-M reports are issued irregularly.

Inquiries about availability of the reports should be addressed to Information Division, Department
of Technical Information, Japan Atomic Energy Research Institute, Tokai-mura, Naka-gun,
Ibaraki-ken 319-11, Japan.

© Japan Atomic Energy Research Institute, 1987

編集兼発行 日本原子力研究所
印刷 山田軽印刷所

A Simple Model for Hot Ion Plasmas

P.R. Thomas*

Department of Large Tokamak Research
Naka Fusion Research Establishment
Japan Atomic Energy Research Institute
Naka-machi, Naka-gun, Ibaraki-ken

(Received April 2, 1987)

This note describes a zero dimensional model for the power balance in the center of tokamaks with additional heating. The main features of the model are classical equipartition and characteristic times, based on L-mode scaling, to represent conductive and convective losses. The model has been tested against data from JET, JT-60 and TFTR. Satisfactory results are obtained if it is assumed that the ions are 3-5 times better confined than the electrons. The good performance of the TFTR "supershots" is found to be associated with the very high power density near to the magnetic axis which is characteristic of these discharges. JET and JT-60, having much lower power densities with NBI alone, can only match the TFTR ion temperatures at lower densities. The performance of JT-60 is predicted to improve markedly if deuterium is used instead of hydrogen.

Keywords: Tokamak, JET, JT-60, TFTR, NBI Heating, Hot Ion Mode, Supershots

* From JET Joint Undertaking, Abingdon, Oxfordshire, U.K.

高イオン温度プラズマの簡易モデル

日本原子力研究所那珂研究所臨界プラズマ研究部

ポール・トーマス*

(1987年4月2日受理)

トカマクにおける追加熱時のプラズマ中心でのパワー・バランスの零次元モデルについて述べる。このモデルは、Lモードに基づく伝導損失及び対流損失を取り入れたものである。まずこのモデルの妥当性をJET、JT-60及びTFTRの実験結果を用いて調べた。イオンの閉じ込めが電子の閉じ込めより3～5倍良いと仮定すると、両者のよい一致を見た。このモデルから、TFTRのスーパーショットの良い閉じ込め特性は、磁気軸近傍における高い加熱密度と関係していることが明らかとなった。加熱密度の低いJETやJT-60では、TFTRのイオン温度を得ようとする、より低いプラズマ密度を必要とする。JT-60の場合には、水素ビームを重水素ビームにかえることによって、大巾な改良が予想される。

Contents

1. Introduction	1
2. The Model	2
3. Comparison with Experiment	5
3.1 JET NBI Data ($d^0 \rightarrow d^+$)	5
3.2 JT-60 NBI Data ($h^0 \rightarrow h^+$)	5
3.3 JET ICRF Data ($(h)^3\text{He}$)	6
3.4 TFTR Supershots	7
3.5 Prediction for JET NBI ($d^0 \rightarrow d^+$)	7
3.6 Prediction for JT-60 NBI ($d^0 \rightarrow \nabla d^+$)	8
4. Conclusions	8
Acknowledgements	10
References	10

目 次

1. 序 論	1
2. モ デ ル	2
3. 実験との比較	5
3.1 JETの中性粒子入射加熱 ($d^0 \rightarrow d^+$)	5
3.2 JT-60の中性粒子入射加熱 ($h^0 \rightarrow h^+$)	5
3.3 JETのイオンサイクロトロン周波数帯加熱 ($(h)^3\text{He}$)	6
3.4 TFTRスーパーショット	7
3.5 JETの中性粒子入射加熱の予測 ($d^0 \rightarrow d^+$)	7
3.6 JT-60の中性粒子入射加熱の予測 ($d^0 \rightarrow \nabla d^+$)	8
4. 結 論	8
謝 辞	10
参考文献	10

A Simple Model for Hot Ion Plasmas

P. R. Thomas

1. Introduction

The substantial fusion yield of the TFTR "supershots" [1] is one of the more impressive features of recent data from the large tokamak experiments. These plasmas produce at 1 MA a neutron flux and estimated d-t yield which exceed those of the larger 3 MA JET plasmas [2]. L-mode confinement scaling [3] would suggest that JET should have the edge, even though TFTR has twice the neutral beam heating power.

It is the improvement in energy confinement over L-mode scaling which is responsible for TFTR's good performance. Whilst it is true that the electron temperature profile broadens in the supershots, so improving the electron energy content, it is primarily in the ions that the energy content resides. In fact, the central thermal ion pressure is sufficiently large in these plasmas that a substantial proportion of the neutron yield is thermonuclear. Many of the experimental conditions for the supershots seem to be directed towards the improvement of the power deposition on axis. For example, the balanced injection might be considered to boost the heating power simply by maximising the relative velocity between the plasma and the fast ions. Likewise, the relatively small plasma currents and the helium discharge conditioning permit the neutral beams to deposit most of the power close to the magnetic axis because the edge density is small.

The purpose of the work to be described in this note was to determine whether a simple model of the central power balance could describe high temperature experiments in JET JT-60 and TFTR not. The details of the model for the thermal insulation of the plasma do not particularly constrain the results. The most important features are classical equipartition and an ion thermal insulation which approximately 3-5 times better than that of the electrons. These two features permit the ions and electrons to be decoupled from each other

and agreement with the temperatures observed in the hot ion mode. It therefore seems that it is the concentration of the heating power on axis which is responsible for the good performance of the supershots. The extent to which the ions are better confined, in this model, than the electrons is strongly constrained by data in which a "hot electron" mode was obtained in JET using hydrogen minority ICRF heating. A somewhat unexpected result is that this data appears to imply that the ICRF is not coupling to the thermal ions except through equipartition with the electrons. A fast minority distribution could not be found to give heating consistent with the data. A possible explanation is that the ICRF is coupling directly to the electrons and this has been used in the modelling. Some predictions for the heating performance of JT-60 with deuterium beam injection onto a deuterium plasma and for JET with 20 MW of beam power are given. In both cases clear hot ion modes can be produced. However the inability to apply the same power density on axis as TFTR will limit the maximum central pressure that can be obtained in JT-60 and JET with neutral beams alone.

The next section describes the model used for the central power balance. After the model is compared with experimental data from JET, JT-60 and JET. Some predictions for JET and JT-60 are given. The last section will present the conclusions of the work.

2. The Model

In order to simulate the central power balance in beam heated plasmas, conduction and convection are represented by separate "confinement" times for the electrons and ions. That is

$$-\frac{n_e T_e \bar{q}}{\tau_e} + Q_e - Q_{eq} = 0 \quad [1]$$

$$-\frac{n_i T_i \bar{q}}{\tau_i} + Q_i + Q_{eq} = 0 \quad [2]$$

$$Q_{eq} = 3.9 \times 10^{-4} n_e \left\{ \sum_j n_j Z_j^2 / m_j \right\} (T_e - T_i) / T_e^{3/2}, \quad [3]$$

and agreement with the temperatures observed in the hot ion mode. It therefore seems that it is the concentration of the heating power on axis which is responsible for the good performance of the supershots. The extent to which the ions are better confined, in this model, than the electrons is strongly constrained by data in which a "hot electron" mode was obtained in JET using hydrogen minority ICRF heating. A somewhat unexpected result is that this data appears to imply that the ICRF is not coupling to the thermal ions except through equipartition with the electrons. A fast minority distribution could not be found to give heating consistent with the data. A possible explanation is that the ICRF is coupling directly to the electrons and this has been used in the modelling. Some predictions for the heating performance of JT-60 with deuterium beam injection onto a deuterium plasma and for JET with 20 MW of beam power are given. In both cases clear hot ion modes can be produced. However the inability to apply the same power density on axis as TFTR will limit the maximum central pressure that can be obtained in JT-60 and JET with neutral beams alone.

The next section describes the model used for the central power balance. After the model is compared with experimental data from JET, JT-60 and JET. Some predictions for JET and JT-60 are given. The last section will present the conclusions of the work.

2. The Model

In order to simulate the central power balance in beam heated plasmas, conduction and convection are represented by separate "confinement" times for the electrons and ions. That is

$$-\frac{n_e T_e \bar{q}}{\tau_e} + Q_e - Q_{eq} = 0 \quad [1]$$

$$-\frac{n_i T_i \bar{q}}{\tau_i} + Q_i + Q_{eq} = 0 \quad [2]$$

$$Q_{eq} = 3.9 \times 10^{-4} n_e \left\{ \sum_j n_j Z_j^2 / m_j \right\} (T_e - T_i) / T_e^{3/2}, \quad [3]$$

where the densities (n_e, n_i) are in 10^{19} m^{-3} , the temperatures (T_e, T_i) in keV, the input power densities (Q_e, Q_i) in $\text{W}\cdot\text{m}^{-3}$ and the electron charge, $\bar{q} = 1.6 \times 10^3$. The subscripts e and i denote electrons and ions. τ_e and τ_i will be defined later.

The electron input power density is given by

$$Q_e = J(0)^2 - \rho_{\text{spitz}} + P_{\text{NB}}(0)(1 - f_i) \quad [4]$$

and the ion power density by

$$Q_i = P_{\text{NB}}(0) f_i \quad , \quad [5]$$

where $P_{\text{NB}}(0)$ is the neutral beam power density on axis, $J(0)$ is the current density on axis assuming $q=1$, ρ_{spitz} is the Spitzer value for electrical resistivity and f_i , which is the fraction of neutral beam power transferred to the ions, given by the Stix [4] formula

$$f_i = \int_0^1 2x dx / (1 + (E_b/E_{\text{cr}})^{3/2} x^3) \quad . \quad [6]$$

E_b is the neutral beam energy and E_{cr} is given by

$$E_{\text{cr}} = 14.8 T_e A_b^{1/3} \{ \sum_j n_j Z_j^2 m_b / m_j / n_e \}^{2/3} \quad , \quad [7]$$

where A_b is the beam particle mass number and the index j runs over the plasma ionic species with charge Z_j .

In order to set a value for the confinement times, τ_e and τ_i , some form must be taken for the variation with scale size, magnetic field and so on. This can be accomplished by eliminating the total power in the L-mode scaling law [3] in favour of the pressure so that

$$\tau_E = 2.91 \times 10^{-3} \beta_T^{-1}(0) \kappa^2 R^{0.5} a^{1.26} (q_a + \alpha_n) q_a^{-2} \quad , \quad [8]$$

where $\beta_T(0)$ is the central toroidal beta ($=2\mu_0 p(0)/\beta_T^2$), κ is the elongation ratio, R the major radius, a the minor radius, q_a is the safety factor and it is assumed that

$$T_{e/i}(r) = T_{e/i}(0) \cdot (1 - (r/a)^2)^{q_a - 1} \quad [9]$$

$$\text{and } n_{e/i}(r) = n_{e/i}(0) \cdot (1 - (r/a)^2)^{\alpha_n} \quad [10]$$

It seems reasonable to assume that the central confinement is not directly affected by the elongation ratio and the profile factors. This gives

$$\tau_E(0) = 2.9 \times 10^{-3} \beta_T^{-1}(0) R^{0.5} a^{1.26} \quad [11]$$

Finally, the somewhat audacious step of asserting that the exponents of R and a are not quite right has been taken. The form used in the model was

$$\tau_{e/i} = f_{e/i} \beta_T^{-1}(0) R a \quad [12]$$

The rationale behind this is that $\beta_T^{-1}(0) a$ should represent the pressure gradient and R the curvature. The effect on the original global scaling is small and could in any case be buried in profile effects. The constants f_e and f_i are found by comparison with data. The best results were found with

$$\begin{aligned} f_e &= 4.2 \times 10^{-4} A_i \\ &= f_i/3 \end{aligned} \quad [13]$$

Unless mentioned otherwise, this is the form of the model used for comparison with the data.

The toroidal beta has a contribution arising from the fast ion pressure. This is given by

$$P_f = 0.08 P_{NB}(0) T_e^{3/2} A_b \mu / n_e Z_b^2 \quad [14]$$

where μ is given by the Stix formula

$$\mu = \int_0^1 x^4 dx / (1 + (E_b/E_{cr})^{3/2} x^3) \quad [15]$$

The equation 1, the electron power balance, was solved using Newton's method and the ion temperature found directly from equation

2. The Stix integrals, equations 6 and 15, were obtained numerically.

3. Comparison with Experiment

3.1 JET NBI Data ($d^0 \rightarrow d^+$)

The JET neutral beam data chosen for this work was a 3 MA, 3.4 T density scan in which the total power was in the range 5 to 7 MW. The conditioning discharges and inner-wall operation were required in order to obtain the lowest densities ($\langle n_e \rangle \sim 1.10^{19} \text{ m}^{-3}$). The highest density plasmas used the outside limiters. The results for the central ion and electron temperature are shown in figure 1. The range in ion temperature reflects the variation due to sawteeth. The solid lines are the results of the model, where it has been assumed that $n_e(0)/\langle n_e \rangle = 1.5$ and the NBI deposition factor $h(0) = 2.5$. The power density on axis was slightly more than $0.12 \text{ MW} \cdot \text{m}^{-3}$. At this low power density, the ions cannot break away from the electrons until the average density is below 2.10^{19} m^{-3} and ion temperature of 12-15 keV are only obtained at 1.10^{19} m^{-3} . The model seems to reproduce the experimental results rather well. The transport coefficient given in equation 13 were fixed using this data.

3.2 JT-60 NBI Data ($h^0 \rightarrow h^+$)

The JT-60 neutral beam data [4] was obtained at 1.5 or 2.0 MA, 4.5 T using hydrogen neutrals onto a hydrogen plasma. The central temperatures are plotted against power at fixed density and density at fixed power in figure 2. In the former case, model curves are shown for $h(0) = 1.35$ and 1.8 whilst for the latter only $h(0) = 1.35$ is shown. The variation was tried in order to assess the effect of the JT-60 beams passing wide of the axis. $h(0) = 1.35$ corresponds to the calculated value and appears to give the better match to the data. $h(0) = 1.8$ is close to the value at the maximum in the deposition profile. The density profiles were taken to be completely flat in the model calculation. It can be seen that the temperatures at the lowest

2. The Stix integrals, equations 6 and 15, were obtained numerically.

3. Comparison with Experiment

3.1 JET NBI Data ($d^0 \rightarrow d^+$)

The JET neutral beam data chosen for this work was a 3 MA, 3.4 T density scan in which the total power was in the range 5 to 7 MW. The conditioning discharges and inner-wall operation were required in order to obtain the lowest densities ($\langle n_e \rangle \sim 1.10^{19} \text{ m}^{-3}$). The highest density plasmas used the outside limiters. The results for the central ion and electron temperature are shown in figure 1. The range in ion temperature reflects the variation due to sawteeth. The solid lines are the results of the model, where it has been assumed that $n_e(0)/\langle n_e \rangle = 1.5$ and the NBI deposition factor $h(0) = 2.5$. The power density on axis was slightly more than $0.12 \text{ MW} \cdot \text{m}^{-3}$. At this low power density, the ions cannot break away from the electrons until the average density is below 2.10^{19} m^{-3} and ion temperature of 12-15 keV are only obtained at 1.10^{19} m^{-3} . The model seems to reproduce the experimental results rather well. The transport coefficient given in equation 13 were fixed using this data.

3.2 JT-60 NBI Data ($h^0 \rightarrow h^+$)

The JT-60 neutral beam data [4] was obtained at 1.5 or 2.0 MA, 4.5 T using hydrogen neutrals onto a hydrogen plasma. The central temperatures are plotted against power at fixed density and density at fixed power in figure 2. In the former case, model curves are shown for $h(0) = 1.35$ and 1.8 whilst for the latter only $h(0) = 1.35$ is shown. The variation was tried in order to assess the effect of the JT-60 beams passing wide of the axis. $h(0) = 1.35$ corresponds to the calculated value and appears to give the better match to the data. $h(0) = 1.8$ is close to the value at the maximum in the deposition profile. The density profiles were taken to be completely flat in the model calculation. It can be seen that the temperatures at the lowest

power levels come out too high in the model and that the electron temperature, at least is reproduced tolerably well above 8 MW. The experimental ion temperature is likely to be an underestimate because it is based on the Doppler broadening of Ti XXI which is not a central species except at low electron temperatures. The correction to give the central ion temperature from this diagnostic is estimated to be in the range 20-50 percent for electron temperatures 2-6 keV (4). Therefore the separation between model and experiment at high temperatures is not particularly worrying and it is suggested that central values of order 9 keV have already been achieved in JT-60. It is important to point out that the mass dependence the transport coefficient in equation 13 is essential for even this level of agreement between model and experiment. When transformed to the more usual form the L-mode scaling the atomic mass appears with a square root dependence. As will be shown shortly, the predictions for deuterium injection on deuterium plasma in JT-60 look far more interesting.

3.3 JET ICRF Data ((h)³He)

This data was obtained at 2 MA, 2.1 T using a generator frequency of 32 MHz. A few percent of hydrogen were added to a ³He plasma a second or so before the RF pulse. The data for the temperatures are shown in figure 3. At low densities, "hot-electron" plasma are produced which also correspond to those with monster sawteeth. Time slices with strong n=2 MHD activity, which usually follows a monster sawtooth collapse, have been suppressed. The model calculations assumed $n_e(0)/\langle n_e \rangle = 1.5$ as before and $h(0) = 5.0$. Modelling these plasmas successfully turned out to be very difficult. A high energy minority distribution would produce very low temperatures because the minority beta was calculated to be large. If the minority beta were removed from the transport model, the temperatures would be reasonable but the magnetic energy contents should have been widely separated from the profile values. A low energy minority distribution caused substantial ion heating and the resulting ion temperatures were much larger than experiment. The only satisfactory model used direct electron heating without an intermediate minority distribution. The

solid lines in figure 3 were generated using this model. The overall behavior was reproduced reasonably well although some slight ion heating would improve the agreement. It is not clear whether the ICRF coupling really is directly to the electrons or not. Some full 1-D modelling would be very useful here. If direct coupling is suggested by transport calculations, this would square well with the absence in the frequency response of the electron temperature of a pole with a time constant around the slowing down time of the minority particles. Instead it is found that there is a pole at about 10 ms which is also the time that it takes for the fast ion tail, observed with the neutral particle analysis to be established. Subject to these qualifications, the ICRF data is reproduced tolerably well.

3.4 TFTR Supershots

As suitable data from a density scan was not to hand, the model was used to calculate the response of the ion and electron temperatures to power at the central electron density of a supershot for which data has been presented [1]. $h(0)=3$ was assumed for this system which has tangential injection. Whilst the neutral beam species mix is not as good as that in JET and JT-60, the peaked density profiles of supershots should make this a reasonable value. The results are shown in figure 4. The calculated temperatures do not appear to be wildly different from those observed in supershots at the 20 MW power level. This serves to underline the importance of power density in TFTR, which approaches $2 \text{ MW}\cdot\text{m}^{-3}$ in the highest power experiments.

3.5 Predictions for JET NBI ($d^0 \rightarrow d^+$)

The predictions for JET beam injection using 80 keV d^0 up to 25 MW are shown in figures 5 and 6. In figure 5 the toroidal beta on axis is plotted against power for three different densities. The fast ion contribution is indicated. The predicted central temperature values are shown against input power for two densities in figure 6. The hot ion mode is only predicted to occur at relatively low

densities compared with TFTR. That notwithstanding, the thermonuclear fusion yield alone is 80% higher at $2 \cdot 10^{19} \text{ m}^{-3}$ than at $4 \cdot 10^{19} \text{ m}^{-3}$. The beam-plasma yield will increase this enhancement factor substantially since the electron temperature is 50% higher at the low density. No enhancement of the central deposition has been assumed in the model predictions. 80 keV deuterium injection gives the largest value of on-axis deposition at an average density of $2 \cdot 10^{19} \text{ m}^{-3}$ in JET. At 120 keV the optimum density is $3 \cdot 10^{19} \text{ m}^{-3}$ and the maximum fusion yield should be obtainable in this region. No attempt has been made to estimate the effect of ICRF heating on the yield but it could be substantial even if the coupling is entirely to the electrons.

3.6 Predictions for JT-60 NBI ($d^0 \rightarrow Vd^+$)

The key issue for JT-60 is the degree to which heating results will change as deuterium is used for both beam injection and plasma species. The mass dependence used in the model guarantees an effect and the results are shown in figure 7. Both electron and ion heating improve even though the same unfavorable deposition profile is assumed. Z_{eff} values of 1 and 2, which are meant to simulate divertor and limiter operation respectively, have been used. The $Z_{\text{eff}}=2$ case gives the higher ion temperature because the pressure is reduced by depletion. However the fusion yield will be higher in the $Z_{\text{eff}}=1$ plasma. This model predicts that the hot ion mode extends to slightly higher densities in JT-60 than JET because the volume is smaller and the main field higher. A big improvement would be obtained if the neutral beams pointed directly at the magnetic axis. It might be worthwhile injecting into small minor radius limiter discharges in an effort to maximise the power density on axis.

4. Conclusions

A model has been developed which describes the heating data from JET, JT-60 and TFTR reasonably well. Since, it is based on the central power balance it is, of course, vulnerable to profile effects,

densities compared with TFTR. That notwithstanding, the thermonuclear fusion yield alone is 80% higher at $2 \cdot 10^{19} \text{ m}^{-3}$ than at $4 \cdot 10^{19} \text{ m}^{-3}$. The beam-plasma yield will increase this enhancement factor substantially since the electron temperature is 50% higher at the low density. No enhancement of the central deposition has been assumed in the model predictions. 80 keV deuterium injection gives the largest value of on-axis deposition at an average density of $2 \cdot 10^{19} \text{ m}^{-3}$ in JET. At 120 keV the optimum density is $3 \cdot 10^{19} \text{ m}^{-3}$ and the maximum fusion yield should be obtainable in this region. No attempt has been made to estimate the effect of ICRF heating on the yield but it could be substantial even if the coupling is entirely to the electrons.

3.6 Predictions for JT-60 NBI ($d^0 \rightarrow \nabla d^+$)

The key issue for JT-60 is the degree to which heating results will change as deuterium is used for both beam injection and plasma species. The mass dependence used in the model guarantees an effect and the results are shown in figure 7. Both electron and ion heating improve even though the same unfavorable deposition profile is assumed. Z_{eff} values of 1 and 2, which are meant to simulate divertor and limiter operation respectively, have been used. The $Z_{\text{eff}}=2$ case gives the higher ion temperature because the pressure is reduced by depletion. However the fusion yield will be higher in the $Z_{\text{eff}}=1$ plasma. This model predicts that the hot ion mode extends to slightly higher densities in JT-60 than JET because the volume is smaller and the main field higher. A big improvement would be obtained if the neutral beams pointed directly at the magnetic axis. It might be worthwhile injecting into small minor radius limiter discharges in an effort to maximise the power density on axis.

4. Conclusions

A model has been developed which describes the heating data from JET, JT-60 and TFTR reasonably well. Since, it is based on the central power balance it is, of course, vulnerable to profile effects,

changing the convection and conduction rates. In spite of that, the experimental values for the central ion temperature are reproduced reasonably reliably by the model, in conditions which are rather different from one machine to the next. In this picture, it is the huge power density on axis in TFTR ($\sim 1.5 \text{ MW} \cdot \text{m}^{-3}$) which is responsible for its superior performance in the hot ion mode. JET ($\sim 0.5 \text{ MW} \cdot \text{m}^{-3}$ at full NBI power) and JT-60 ($\sim 0.6 \text{ MW} \cdot \text{m}^{-3}$) only come close to matching TFTR ion temperatures because of their superior thermal insulation. In neither case could the hot ion mode be obtained at as high a density as TFTR unless the ratio of peak to volume average density is radically improved in both machines. The natural advantage that tangential injection brings would appear to be difficult to surpass because it makes the "deposition instability" more likely. The predictions point to both JET and JT-60 attaining ion temperatures of 15-20 keV at $2-3 \times 10^{19} \text{ m}^{-3}$ with the flattish density profiles characteristic of both machines.

The mass dependence of the thermal insulation is required in the model in order that the heating results in JT-60 can be matched to those of JET and TFTR. Since this is in accord with the experience of small machines it would seem likely that JT-60 will see a major improvement in performance once permission is granted to use deuterium. In addition there will be some improvement of the power deposition on axis although this will be a relatively small effect.

The confinement model used here is not crucial to the findings concerning heating in the large tokamaks. The most important requirements are that the ions be better insulated than the electrons together with equipartition being classical. However, some features of the model are observed in experiments. In particular, the model has the thermal energy content independent of density at high power as shown in figure 5. Also, the model is capable of producing an energy content which at high density is linear with power, as seen in the same figure.

The suggestion that the ICRF couples directly to the electrons in JET, whilst not completely out of the question, is peculiar and should be investigated further. There are already indications that the minority species is not playing the role anticipated of it in the power modulation experiments.

The work described here must be regarded as a "scoping exercise" and some of the findings should be investigated in greater detail. The next step to be taken will be to determine the conditions under which the maximum d-t fusion yield could be obtained given the assumptions here. In particular the advantages of the hot ion mode relative to full thermalisation in reaching the JET programme goals will be assessed.

Acknowledgements

The work described here was performed whilst the author was visting JT-60 under the auspices of the IEA Cooperation Agreement between JET, JT-60 and TFTR. It is a pleasure to acknowledge the hospitality of the JT-60, Large Tokamak Experiment division and Y. Shimomura, and S. Tsuji in particular. The author is grateful for useful conversations concerning this work with M. Kikuchi, M. Nagami and M. Bell (TFTR).

References

1. R. J. Hawyluk et al., XI th International Conference on Plasma Physics and Controlled Thermonuclear Fusion, Kyoto 1980.
R. J. Goldston et al., *ibid*.
2. To appear in a JET preprint
3. R. J. Goldston, Plasma Physics and Controlled Fusion 26 (1984) p87.
4. JT-60 team, JAERI-M report 87-009 (1987).

The work described here must be regarded as a "scoping exercise" and some of the findings should be investigated in greater detail. The next step to be taken will be to determine the conditions under which the maximum d-t fusion yield could be obtained given the assumptions here. In particular the advantages of the hot ion mode relative to full thermalisation in reaching the JET programme goals will be assessed.

Acknowledgements

The work described here was performed whilst the author was visting JT-60 under the auspices of the IEA Cooperation Agreement between JET, JT-60 and TFTR. It is a pleasure to acknowledge the hospitality of the JT-60, Large Tokamak Experiment division and Y. Shimomura, and S. Tsuji in particular. The author is grateful for useful conversations concerning this work with M. Kikuchi, M. Nagami and M. Bell (TFTR).

References

1. R. J. Hawyluk et al., XI th International Conference on Plasma Physics and Controlled Thermonuclear Fusion, Kyoto 1980.
R. J. Goldston et al., *ibid.*
2. To appear in a JET preprint
3. R. J. Goldston, Plasma Physics and Controlled Fusion 26 (1984) p87.
4. JT-60 team, JAERI-M report 87-009 (1987).

The work described here must be regarded as a "scoping exercise" and some of the findings should be investigated in greater detail. The next step to be taken will be to determine the conditions under which the maximum d-t fusion yield could be obtained given the assumptions here. In particular the advantages of the hot ion mode relative to full thermalisation in reaching the JET programme goals will be assessed.

Acknowledgements

The work described here was performed whilst the author was visting JT-60 under the auspices of the IEA Cooperation Agreement between JET, JT-60 and TFTR. It is a pleasure to acknowledge the hospitality of the JT-60, Large Tokamak Experiment division and Y. Shimomura, and S. Tsuji in particular. The author is grateful for useful conversations concerning this work with M. Kikuchi, M. Nagami and M. Bell (TFTR).

References

1. R. J. Hawyluk et al., XI th International Conference on Plasma Physics and Controlled Thermonuclear Fusion, Kyoto 1980.
R. J. Goldston et al., *ibid.*
2. To appear in a JET preprint
3. R. J. Goldston, Plasma Physics and Controlled Fusion 26 (1984) p87.
4. JT-60 team, JAERI-M report 87-009 (1987).

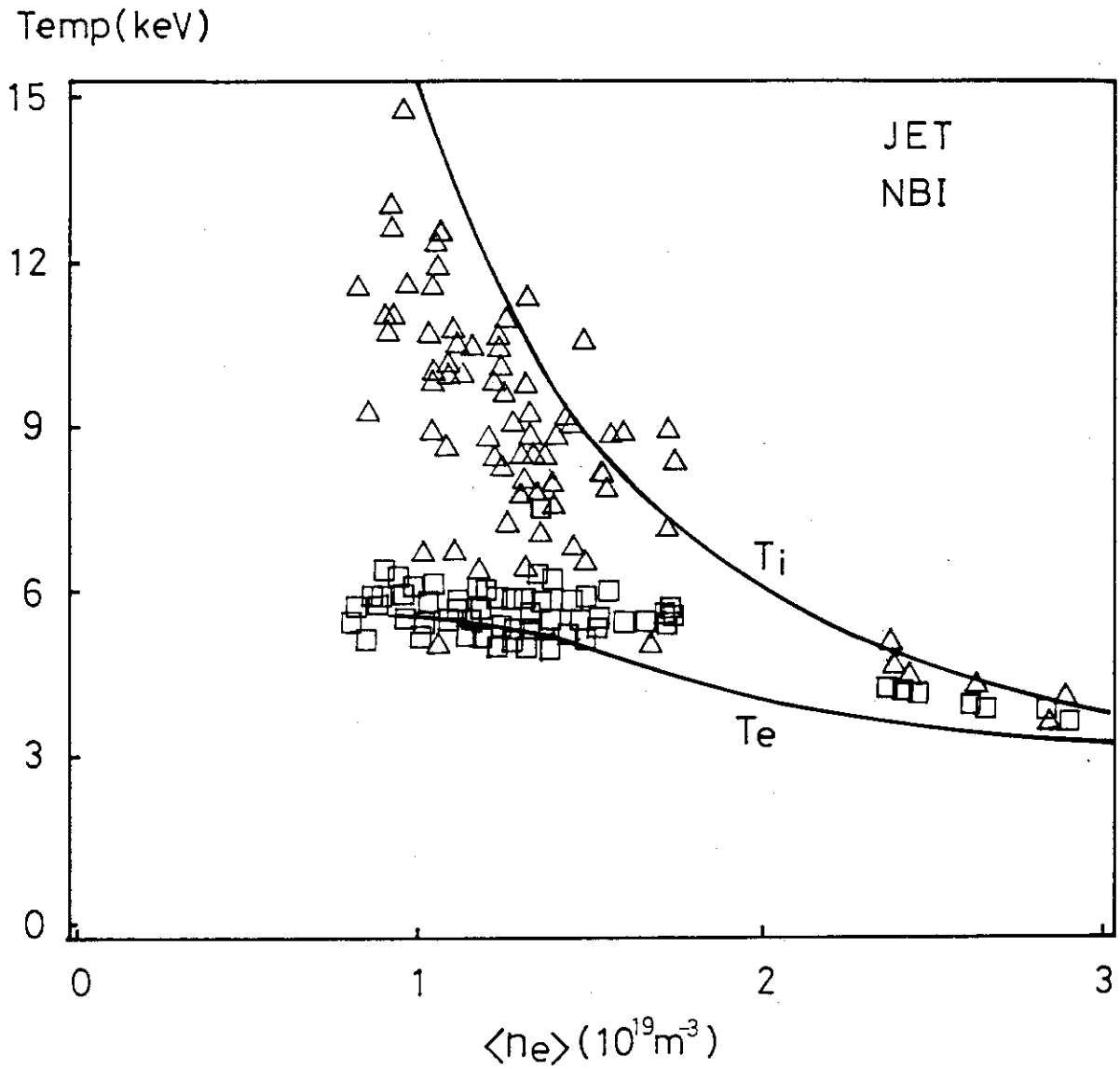


Fig.1

Central electron (\square) and central ion (Δ) temperatures against volume average density for JET 3MA/3.4T $d^0 \rightarrow d^+$ NBI plasmas with $5.0 < P_{tot} < 7.0$ MW. The simulation assumes $h(0) = 2.5$ and $n_{eo} / \langle n_e \rangle = 1.5$

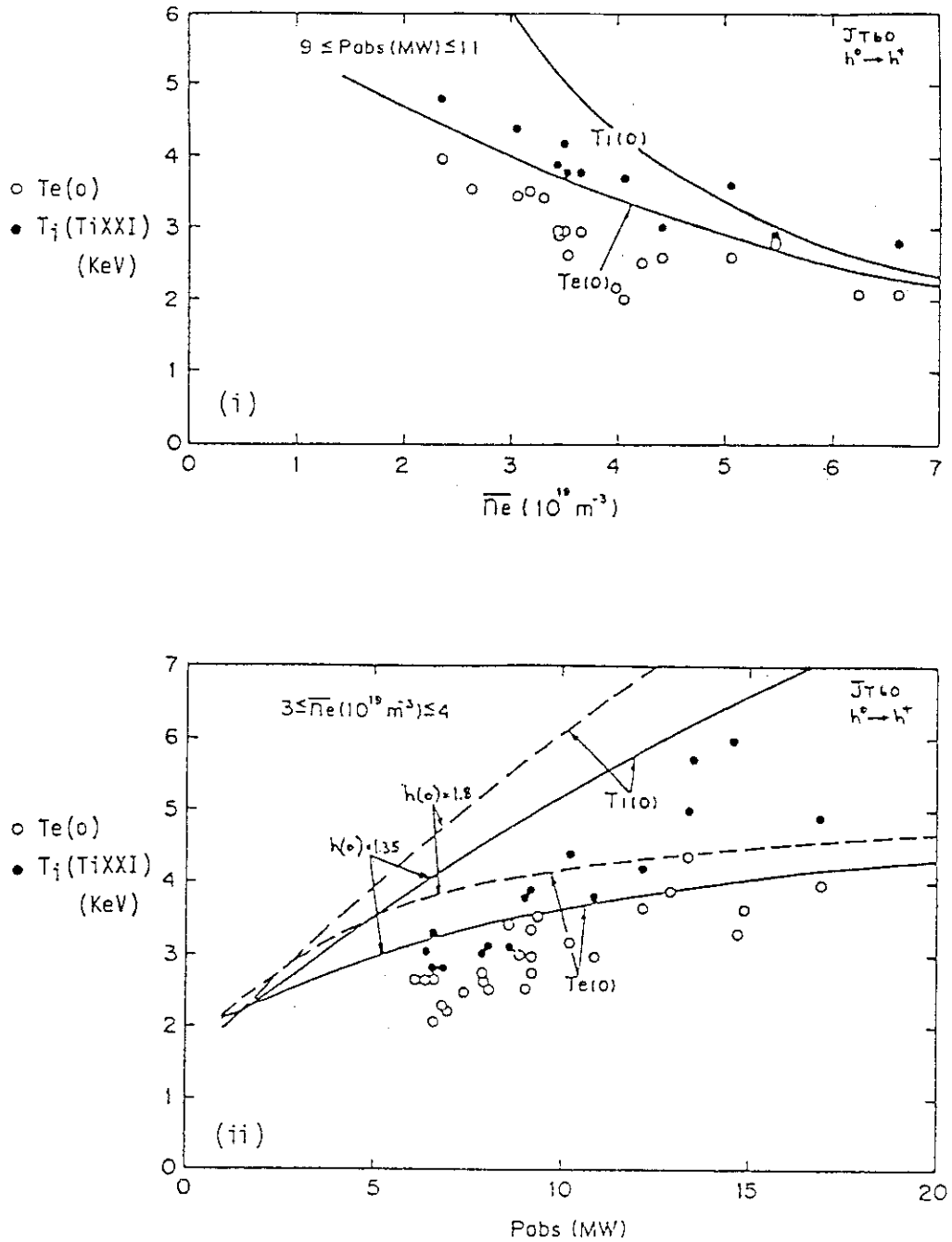


Fig.2

JT-60 $h^0 \rightarrow h^+$, 1.5 - 2.0MA, 4.5T plasmas: (i) shows central temperatures against average density at fixed power, whilst (ii) shows central temperatures against power at fixed average density. The model results are shown with the solid lines. Flat density profiles were assumed with $Z_{\text{eff}} = 1$. (ii) shows the effect of a more peaked deposition profile.

Temp (keV)

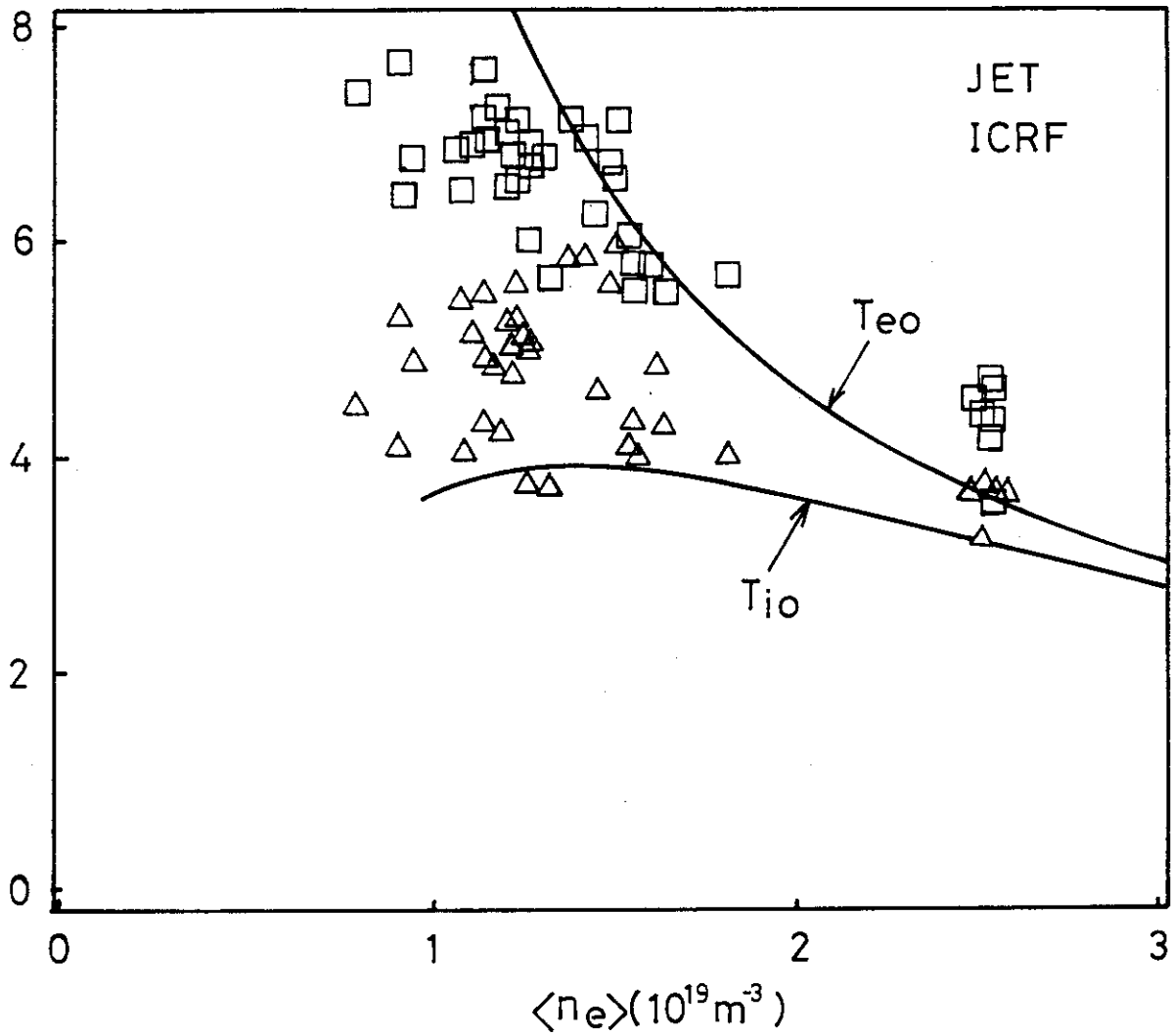


Fig.3

Central electron (\square) and central ion (Δ) temperatures against volume average density for JET 2MA/2.1T (h) ^3He ICRF plasmas with $5.0 \leq P_{\text{tot}} \leq 7.0$ MW. The simulation assumes direct coupling of the RF to the electrons and $n_{e0}/\langle n_e \rangle = 1.5$

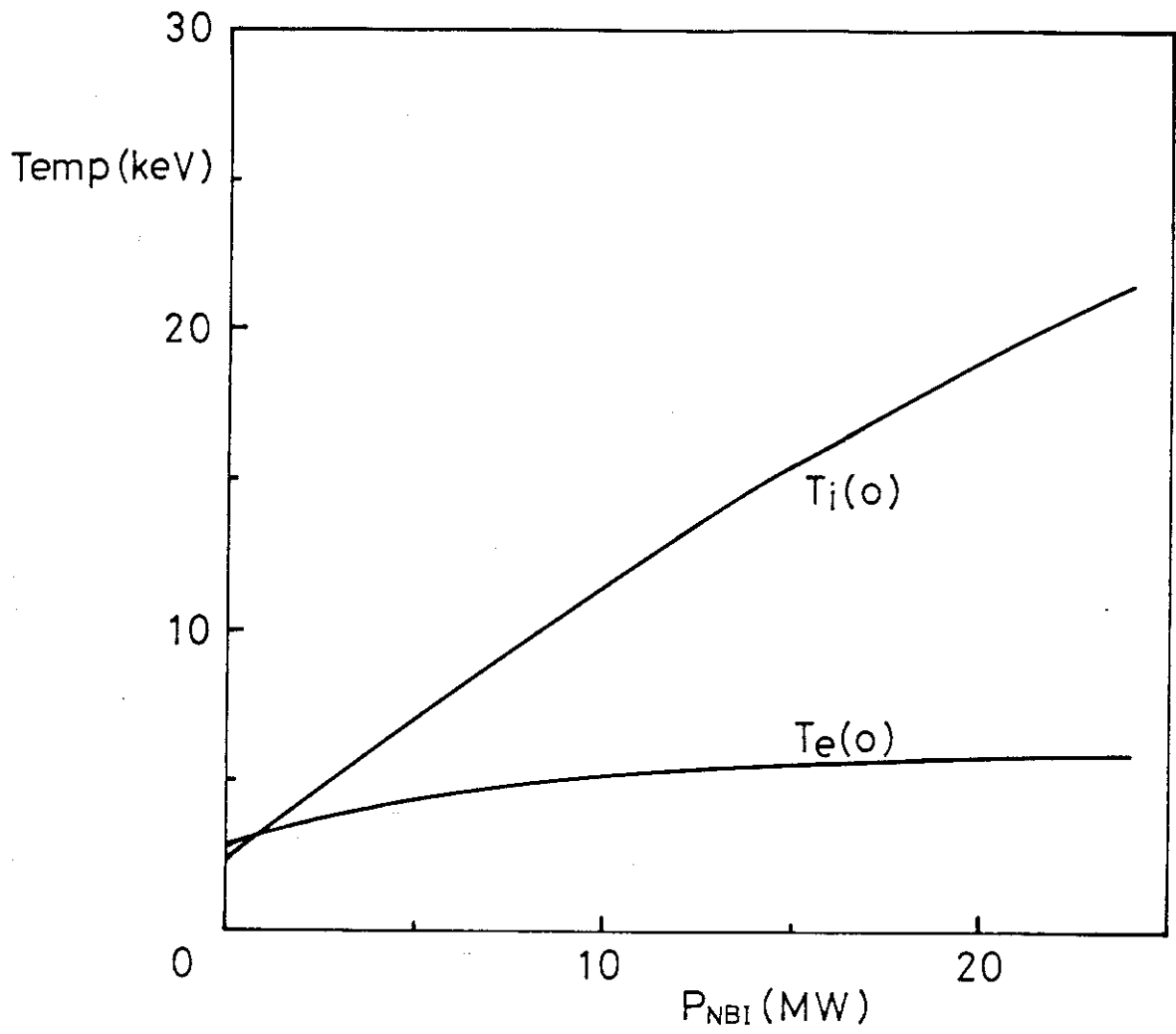


Fig.4

Model results for TFTR. $h(o) = 3$, $n_e(o) = 6 \cdot 10^{19} \text{ m}^{-3}$, $Z_{\text{eff}} = 2$ and $B_T = 5T$ have been taken.

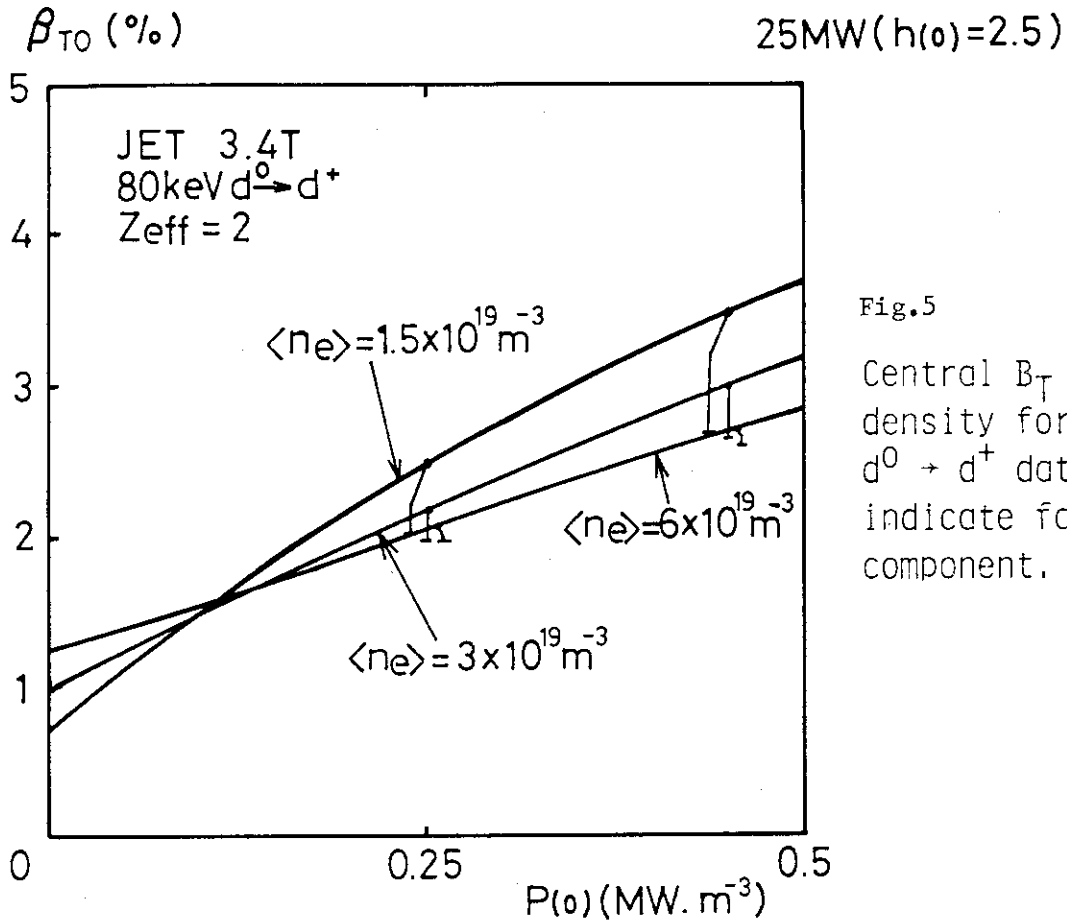


Fig.5

Central β_T against power density for JET 3.4 T $d^0 \rightarrow d^+$ data. Bars indicate fast ion component.

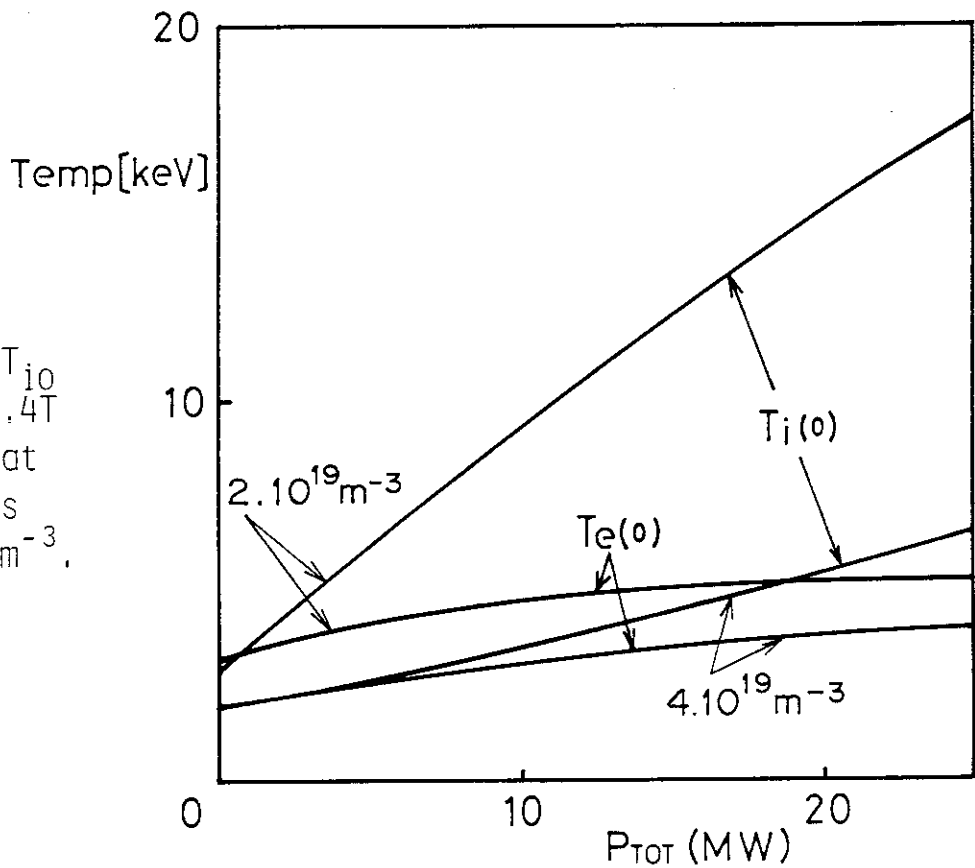


Fig.6

Predictions for T_{i0} and T_{e0} in JET 3.4T $d^0 \rightarrow d^+$ plasmas at average densities of 2 and $4 \cdot 10^{19} \text{ m}^{-3}$.

Temperature (keV)

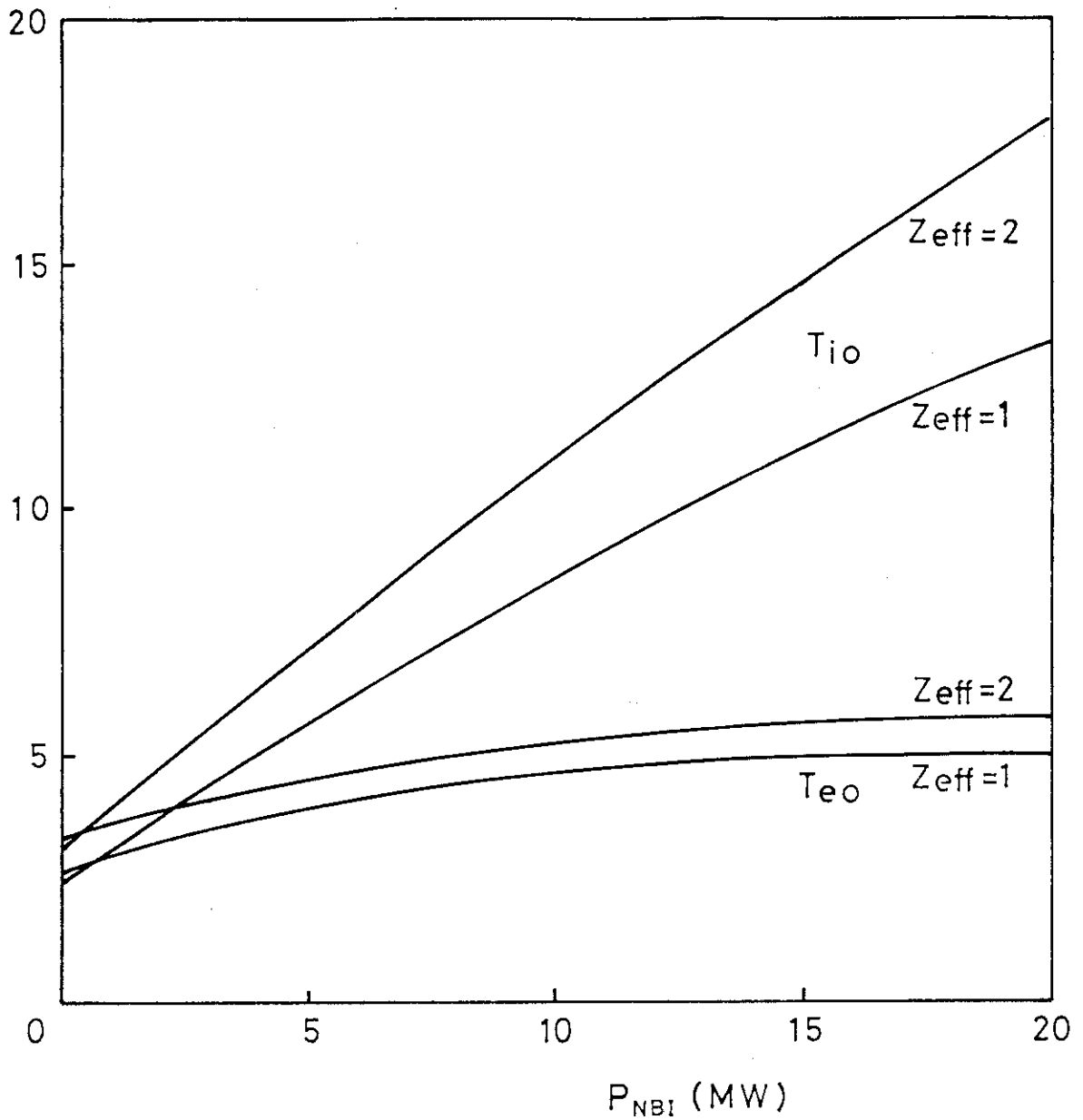


Fig.7

The predicted central ion and electron temperatures at $n_{e0} = 3.5 \times 10^{19} \text{ m}^{-3}$ for JT60 with $d^0 + d^+$ NBI at 4.5 T. Predictions for $Z_{\text{eff}} = 1$ and 2 are shown.